Effect of Tip Injection on an Axial Compressor using Airflow Recirculation - Numerical Investigations

Melanie Achmus, Nils Budziszewski, Jens Friedrichs, Henner Schrapp

Effect of Tip Injection on an Axial Compressor using Airflow Recirculation - Numerical Investigations

Melanie Achmus[1]*, Nils Budziszewski[1], Jens Friedrichs[1], Henner Schrapp[2]

ISROMAC 2016

International Symposium on Transport Phenomena and Dynamics of Rotating Machinery

Hawaii, Honolulu

April 10-15, 2016

Abstract

In this paper the results of a numerical analysis concerning the impact of a passive flow control technique on a 1.5-stage axial compressor are presented. In order to examine the effects occurring due to the application of discrete tip blowing in the rotor domain, unsteady flow simulations are conducted. In low speed axial compressors the rotor blade tip area is critical concerning the effect of flow separation because of low momentum fluid in the endwall boundary layer and the rotor tip leakage vortex. These flow effects cause a loss in efficiency and are furthermore responsible for a cutback in the compressor working range. As a potential method to increase the working range the impact of recirculation ducts in the rotor casing is investigated in this study. Due to the static pressure gradient over the rotor passage fluid flows through the recirculation ducts, reenergizing the boundary layer at the leading edge of the rotor tip. Their design and positioning take the limited available space in aeroengines into account. This survey focuses on the impact of the tip blowing jet on the rotor performance, in particular the interaction of the recirculated mass flow and the tip leakage vortex will be discussed.

Keywords

tip injection — performance enhancement — stability improvement — flow recirculation

[1] *Institute of Jet Propulsion and Turbomachinery, Technical University Braunschweig, Germany*

[2] *Rolls-Royce Deutschland Ltd & Co KG, Blankenfelde-Mahlow, Dahlewitz, Germany*

*__Corresponding author__: m.achmus@ifas.tu-bs.de

INTRODUCTION

The design of modern axial compressors for jet engines is driven by the striving for an increase in overall pressure rise at constant or even higher efficiencies. The resulting increase in aerodynamic loading leads to a reduction in surge margin. In modern axial compressors the tip leakage flow, streaming through the rotor tip gap due to the difference in pressure between suction and pressure side, usually is the reason for stall inception. The tip leakage flow starts to spin and evolves into the tip leakage vortex, which is a major source of losses in compressors and is responsible for the decrease of pressure rise and efficiency at low flow coefficients. With decreasing flow coefficients the tip leakage vortex shifts upstream. Eventually the tip clearance flow spills into the neighboring passage and thereby even crosses the leading edge plane of the blades [1]. This situation is called spill forward and is considered to be a main origin of spike type stall inception. Manipulating the tip leakage vortex to such a degree as the upstream shifting of the vortex is postponed to even lower flow coefficients, the operating range can be increased. Influencing the boundary layer at the rotor shroud and therefore the tip leakage vortex by tip blowing is considered to be a promising possibility of increasing the surge margin. A distinction is made between active and passive ways to accomplish tip blowing in aero engines. Active methods include valves and feedback control systems and have shown to more efficiently counteract stall inception [2]. However, it leads to an increase in complexity and costs. Considering durability and reliability passive methods are more suitable for application in aero engines. This advantage causes an increase in research on passive re-injection. Driven by the pressure difference fluid is recirculated from a downstream position to a stall critical location, usually near the rotor leading edge. A crucial point concerning the effectiveness of tip blowing is the position at which the fluid is injected. The impact of the tip blowing location or size on compressor performance has been investigated in several studies [3–6], yet it is difficult to draw general conclusions, as the mechanisms of stall inception vary from one compressor to another [2, 7]. In order to gain a deeper understanding for the effects and mode of action of tip blowing, studies are made concerning fully annular injectors [4, 8–10] as well as discrete injection ports [3, 6, 7, 11–15]. The advantage of discrete injection is that re-recirculation can be avoided. In addition it was discovered, that the periodic excitation of the tip leakage vortex by discrete injection can damp stall generating modal waves [14]. It is generally agreed that recirculation has the ability to increase the stall margin. It has been found, that the improvement in stall range increases with increasing injected mass flow [7, 8]. Yet, the losses which occur due to the fact that there are friction losses in the duct, rise when increasing the amount of recirculated mass flow. Khaleghi [15] did a numerical study on the effect of tip blowing on a single rotor row using recirculation ducts for a very small amount of recirculated fluid (less than 0.2 percent of the annulus mass flow). It could be shown that even a very small amount of recirculated mass flow leads to a range extension. Yet, this range extension is accompanied by a deterioration of rotor performance, albeit a minor one, in design conditions.

However, in many studies an external air supply is used to generate the tip blowing mass flow. These approaches run the risk of underestimating the cutback in efficiency at design conditions due to recirculation. In this study the effect of discrete tip blowing using recirculation ducts is analyzed. This realistic approach does not only record the predominant beneficial aerodynamic effect of tip blowing but, concerning the compressor performance, it also includes the extraction of compressed air at the rotor trailing edge. Unlike in [15] the number of rotor blades is double the number of ducts, the cross sectional area of the duct varies and it does not penetrate into the flow field. Its behavior is computed in a 1.5-stage compressor configuration operating in subsonic speeds.
The focus of this study is not only on the change in operating range but also on the interaction of recirculated mass flow and tip leakage vortex at near stall and design conditions.

1. SIMULATION MODEL

The current subsonic compressor stage was analyzed numerically as well as experimentally. The numerical study was performed using unsteady flow simulations. Within this study, the aerodynamic characteristics of the smooth casing configuration and the ducted configuration at design speed are compared. To ensure comparability of the numerical studies the smooth casing configuration was treated as an unsteady flow problem as well.

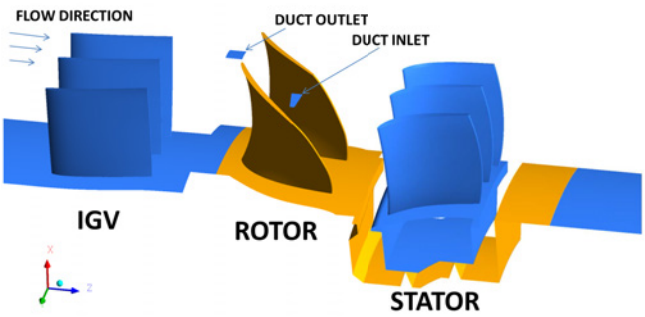

Figure 1. Numerical Setup

The numerical simulation covers the 1.5-stage axial compressor setup, shown in Fig. 1. The numerical model and the analyzed experimental setups differ in the rotor tip clearance. While in the experimentally examined setups the gap between rotor tip and shroud were 1% and 3% of the annulus height, the rotor tip clearance in the numerical model is 1.7%. At the time of writing, the experimental results of the 1.7% tip clearance configuration were not yet available. Due to this difference, a direct comparison between the experimental and numerical results is not possible. However, the resulting tendencies concerning the impact of tip blowing on the compressor characteristic are transferable.
For the numerical study Ansys CFX has been applied. The meshing was implemented using Numeca Autogrid, generating structured meshes for the entire passage geometry. Merely small parts of the recirculation ducts, which will be discussed later on, were meshed unstructured by means of ICEM CFX. A mesh study was executed, resulting in a mesh with a size of 189.5 million nodes for the 360 degree model and thus 12 million nodes for the numerical setup shown in Fig. 1. As a preliminary assessment a refinement of the depicted setup ranging from 4.1 to 14.5 million nodes was realized. Subsequently the influence of coarsening and refining separate domains on the stage performance was examined. A number of 1.3 million nodes for a single IGV domain (including the inlet channel), 1.39 million nodes for a rotor domain and 1.78 million nodes for a stator domain (including the stator cavity) proved to be appropriate. To ensure good solutions for the tip blowing and flow extraction area, special attention was given to the meshing of the shroud sector of the rotor domain. For turbulence simulation the SST model has been used. Based on a y^+ criterion wall functions were automatically applied. The inlet boundary conditions were defined by the total temperature and the total pressure, the outlet boundary condition was defined by the mass flow rate.

The intention of the flow simulation was to create a model of the test facility which is as close to reality as possible. That is why the numerical model includes the complete 1.5 stages consisting of IGV, rotor and stator as well as stator cavity and recirculation ducts. For that purpose the wide-stretched inlet channel is also included in the model. For a better viewing of the blades, the inlet channel is not depicted in Fig. 1.
The simulation of a rotor blade passage with discrete flow injection necessitates time-accurate flow simulations, due to the fact that the rotor passes the duct inlet and outlet. To consider the effect of the wakes on the flow through the downstream blade passages, not only the interfaces in the rotor domain but each interface is defined as time-accurate. Yet, the unsteady flow simulation of the present configuration requires some modifications of the model, which will be discussed below.
A simulation of a combination of 29 rotor blades and 16 recirculation ducts, which is analyzed in the experimental setup, is only possible with a 360 degree model of the domain. Thus to keep computing time in a reasonable limit a model containing 30 rotor blades and 15 recirculation ducts is used. The geometry of the rotor blades was adapted using domain scaling. This way the pitch to chord ratio remains the same and there is no more than a marginal change in stage characteristics [16, 17]. The recirculation duct was rescaled so that a number of 15 scaled ducts recirculate the same amount of fluid as 16 original ducts.
For a one-to-one transfer of the flow conditions from one side of the interface to the other a pitch ratio of one is required. The simulated numerical model is composed of three IGV blades, two rotor blades in combination with one recirculation duct and three stator blades, as shown in Fig. 1. The resulting pitch ratio is 0.9375. Therefore the wakes are slightly stretched or shrinked at the domain interfaces. As the main intention in this publication is to analyze the interaction of recirculated mass flow and tip gap vortex rather than considering wake interactions and frequencies, these distortions are regarded as

tolerable concerning the current study.
The interface connecting the rotor domain to the recirculation duct inlet and outlet is realized using the Sutherland-Hodgman-Algorithm. The recirculation duct is compound of three parts. The main part consists of a structured, 0.29 million nodes mesh. To allow high mesh quality the very back acute-angled edges of the duct inlet and outlet are realized each with an unstructured tetrahedron mesh.
The time-accurate flow simulations were performed using 150 timesteps for a 24 degree rotation of the rotor domain. This corresponds to two rotor blades passing one recirculation duct and thus to the time of the periodic sequence. The number of inner iterations was triggered by a target residual of $3 \cdot 10^{-5}$ and a maximum number of 10 iterations. The timestep size and the number of inner iterations was edited so that the limit of 10 iterations was rarely reached. For the timestep size a value of $9.44 \cdot 10^{-6}$ seconds was chosen. This way the root mean square of the Courant number, which describes the number of cells flown through by a fluid particle during one timestep, is 6.5. To determine the convergence of the unsteady calculations, the temporal evolvement of flow parameters at various locations inside the model were monitored. The efficiency and the total pressure ratio were used as a main indicator for convergence. Exemplarily the course of efficiency and total pressure ratio of a converged solution is shown in Fig 2.

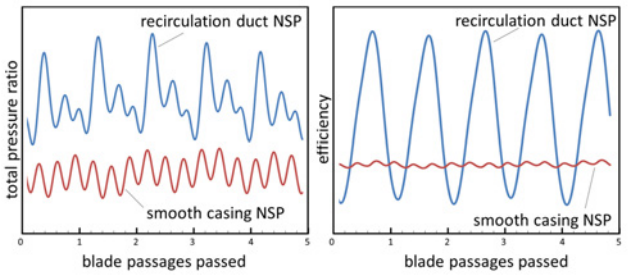

Figure 2. Time Variation of Total Pressure Ratio and Efficiency at NSP

2. RESULTS

2.1 Effect of Recirculation Ducts on Operating Range

In Fig. 3 a comparison between the stage performance of the experimental results and two numerically obtained operating points is drawn. The two numerical operating points shown are those points which will in the following sections be discussed in more detail. In the scope of the experimental investigations a rotor tip clearance (TCL) of 1% and 3% were analyzed. The numerical data is available for a TCL of 1.7%. To get a clear view of the differences between the analyzed points, an enlarged view is shown which does not include the stall and choke area. The data has been normalized with the respective numerical value at the design point of the smooth casing configuration. As can be seen in Fig. 3, the prediction of total pressure rise lies in a satisfying range. Even if the

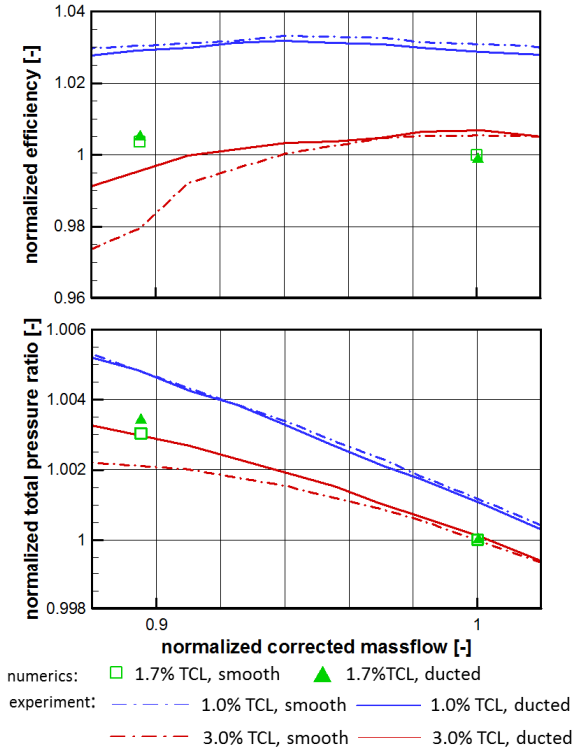

Figure 3. Efficiency and Total Pressure Ratio Characteristic of the complete Stage

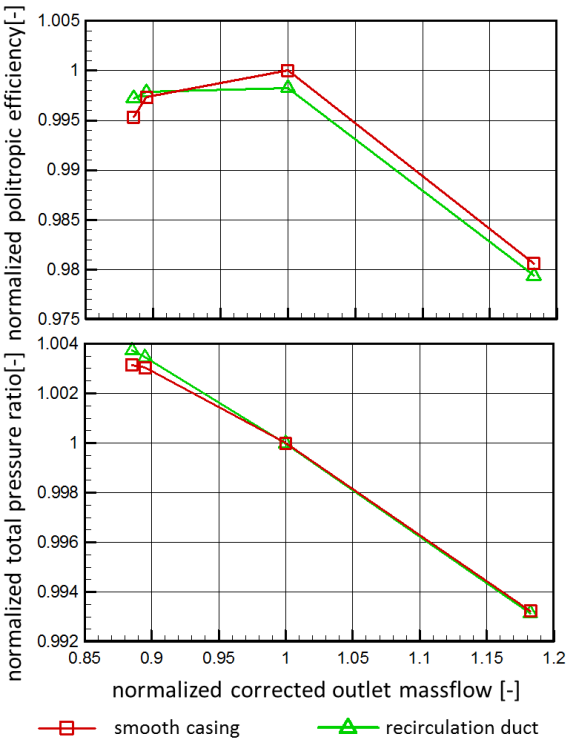

Figure 4. Efficiency and Total Pressure Ratio Characteristic of the Rotor Domain

calculated pressure rise is nearer to the 3% characteristic than to the 1% characteristic, its deviation from its expected (interpolated) position is less than 0.085% for every calculated point. The prediction of the efficiency is less accurate. The values for the efficiency are underrated by 1.6% on average. Comparing the characteristics of the ducted and the smooth casing configuration it gets apparent that recirculation is profitable at larger TCLs. For a TCL of 1% the efficiency of the ducted configuration is lower than the efficiency of the smooth casing configuration. There is nearly no difference in pressure rise. Concerning the 3% TCL configuration, the efficiency of the ducted configuration is consistently higher than the efficiency of the smooth casing configuration. The pressure ratio shows a more continuous rise and higher values for the ducted configuration. Based on the numerical data the transition from a more negative to a positive impact of the duct can be observed. While the performance at design conditions is still better for the smooth casing configuration, this situation changes at lower mass flow rates. The change in efficiency and pressure ratio due to recirculation for a TCL of 1.7%, which is expected based on interpolation of the experimental data, matches very well with the numeric results. The improvement of stage performance starts at the stall area of the characteristic and stretches out to higher mass flow rates with increasing TCL. The impact of tip blowing on the rotor performance at 1.7% TCL is shown in Fig. 4. In this figure only the rotor passage is considered. In the most throttled operating point available the gain in efficiency is 0.19% compared to the smooth casing configuration. The characteristics indicate that there is an increase in surge margin induced by the recirculation ducts. However, due to the small number of available operating points, the actual increase in surge margin cannot be determined. Regarding the design point and the operating point at high mass flow rates it gets apparent that at the current TCL, the advantage of the recirculation ducts takes effect only at the stall region of the characteristic. For the efficiency as well as for the total pressure rise in the throttled operating points, lower values are achieved with the ducted configuration. The calculated loss in efficiency at the design point is 0.17%.

The question arises which factors cause the positive impact on the aerodynamic characteristics in the stall range and which effects are responsible for the negative impacts at high mass flow rates. That is why in the following a closer look at the interaction between recirculated massflow and rotor leakage flow is taken.

2.2 Time Averaged Radial Profiles of Flow Parameters

In this section, the effect of recirculation on the flow conditions at the rotor outlet plane is discussed. Radial profiles of total pressure, efficiency and loss coefficient at the design point (DP) and a near stall operating point (NSP) are analyzed. The radial contours (Fig. 5 to Fig. 6) are circumferentially averaged, time averaged and normalized with the smooth casing configuration value at design conditions at 50% annulus height.

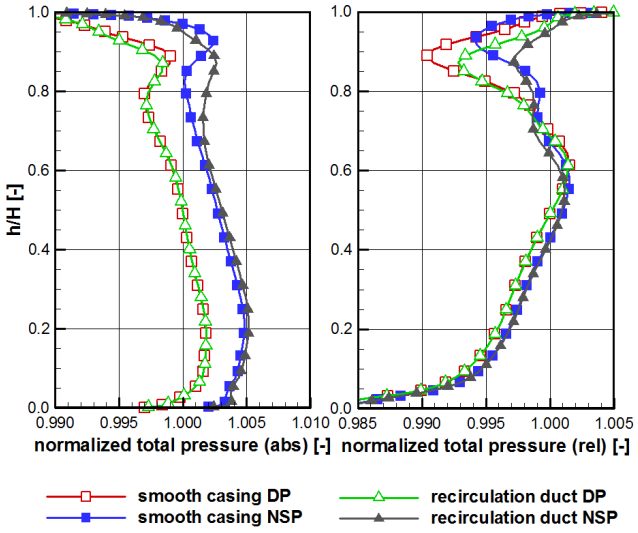

Figure 5. Radial Profiles of Normalized Total Pressure in Relative and Absolute Frame of Reference, Rotor Outlet Plane

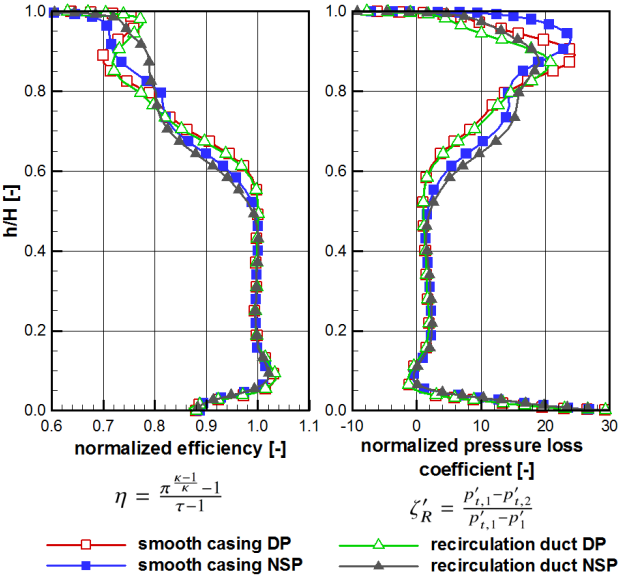

Figure 6. Radial Profiles of Normalized Isentropic Efficiency and Normalized Pressure Loss Coefficient, Rotor Outlet Plane

Comparing the course of the total pressure in Fig. 5 it can be seen that in the lower two thirds of the annulus tip blowing leads to a higher total pressure in the absolute frame of reference and to a slightly lower or equal total pressure in the relative frame of reference. As the total pressure correlates with the velocity, this implies a higher deflection concerning the ducted configuration. Getting closer to the shroud another effect shows. Near the shroud, from about 90% annulus height, tip blowing leads to a lower total pressure in the stationary frame of reference, but to a higher total pressure in the relative frame of reference. This implies a reduced deflection at the rotor tip area. It is assumed, that this loss in deviation angle is

caused by the axial momentum of the injected flow. Since a reduced deflection is equivalent to an aerodynamic unloading of the blade, smaller loss coefficients are recorded in this area, as can be seen in Fig. 6. With increasing distance to the shroud the ducted configuration records a higher deflection in the relative frame of reference and thus slightly higher loss coefficients. Since the flow angles at the rotor domain inlet do not change, this implies that due to the tip blowing jet the aerodynamic loading of the rotor blades decreases in the tip area. The aerodynamic loading is shifted towards the mid of the annulus.

The shape of the radial profiles of rotor efficiency and pressure loss coefficient, shown in Fig. 6, correlate with each other. A smaller pressure loss coefficient implies a higher efficiency. Comparing the average values it becomes apparent that a decrease of pressure loss coefficient does not necessarily involve an increase in efficiency, since the pressure loss coefficient is a quantity obtained from the relative frame, whereas the efficiency is a quantity obtained from the stationary frame of reference. While at the near stall operating point for the ducted configuration the average efficiency is higher and the average pressure loss coefficient is lower, at design conditions the average loss coefficient is lower while the average efficiency is lower as well. Thus concerning the design point the losses in the relative frame of reference are lower, while the losses in the stationary frame of reference are higher. Concerning the design point, tip blowing using the recirculation ducts causes an aerodynamic improvement in the relative frame of reference, yet the efficiency slightly decreases.

2.3 Impact of Tip Blowing Jet on Tip Leakage Vortex

Fig. 7 and Fig. 8 show three different snapshots of the static pressure contour for the ducted and for the smooth casing configuration respectively. Figure 7 shows the contour at design conditions, Fig. 8 shows the contour at near stall conditions. The contours of each figure have been plotted in the same range. The pictured values have been normalized each with the maximum value. For each snapshot the flow topology was recorded in the same fixed axial oriented plane (compare Fig. 10). The plane is positioned in such way that it runs through the mid of the recirculation duct outlet. The snapshots were taken with a real time lag of 9.44 and 18.88μs respectively, in which a part of the rotor passes the duct. The examined area is at the front third of the rotor blade. The adjacent snapshots of the ducted and the smooth casing configuration were taken at the same local position and each at the same relative position of recirculation duct and rotor blade.

Comparing the associated static pressure contours at the near stall operating point (Fig. 8) the impact of the tip blowing jet on the development of the tip leakage vortex can be identified. While the vortex, which can be identified as an area of very low static pressure near casing at the suction side of the blade, is relatively near to the blade surface when applying recirculation, it spreads further to the blade passage without the effect of tip blowing. The tip blowing jet apparently successfully prevents

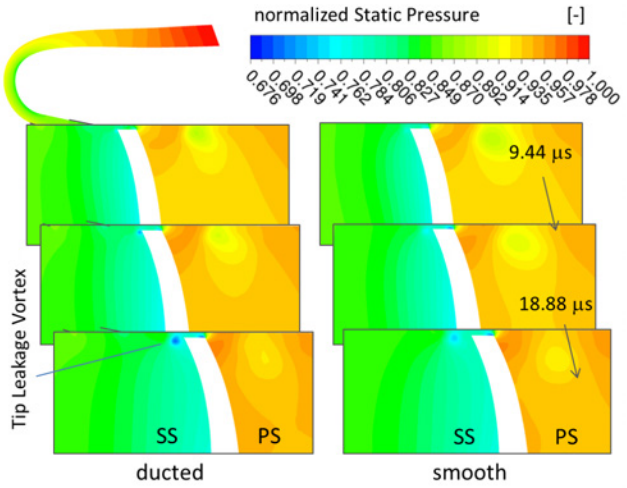

Figure 7. Static Pressure Contours at DP for Ducted and Smooth Casing Configuration

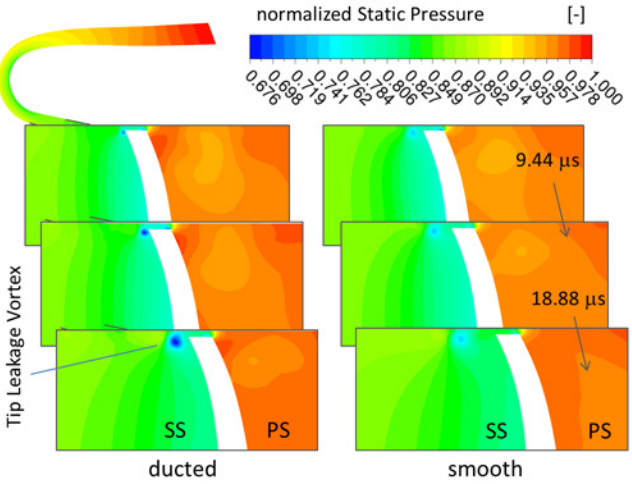

Figure 8. Static Pressure Contours at NSP for Ducted and Smooth Casing Configuration

the tip leakage vortex from circumferentially propagating into the blade passage.

Furthermore, the ducted configuration shows a lower static pressure in the vortex center, which indicates a higher rotational speed. This effect is less distinct at design conditions. Concerning the formation of the vortex equal tendencies can be observed, but the entire vortex is smaller in size and intensity. This is due to the fact that at less throttled operating points the vortex forms further downstream because of the lower pressure gradient between pressure side and suction side. This is an explanation for the little positive effect of the duct on the aerodynamic characteristics at design conditions and near choke conditions. It is not only that the recirculated mass flow is smaller due to the lower pressure gradient between the duct inlet and the duct outlet, but also that the jet is injected farther from the origin of the tip leakage vortex.

For this reason the tip leakage flow and the tip blowing jet do not interact in an optimum way. The impact of the tip blowing jet on the formation of the leakage vortex is smaller. In this case negative effects, as for example the extraction and recirculation of compressed air or the occurring losses inside the duct dominate the positive effects of the tip blowing and cause a lower efficiency.

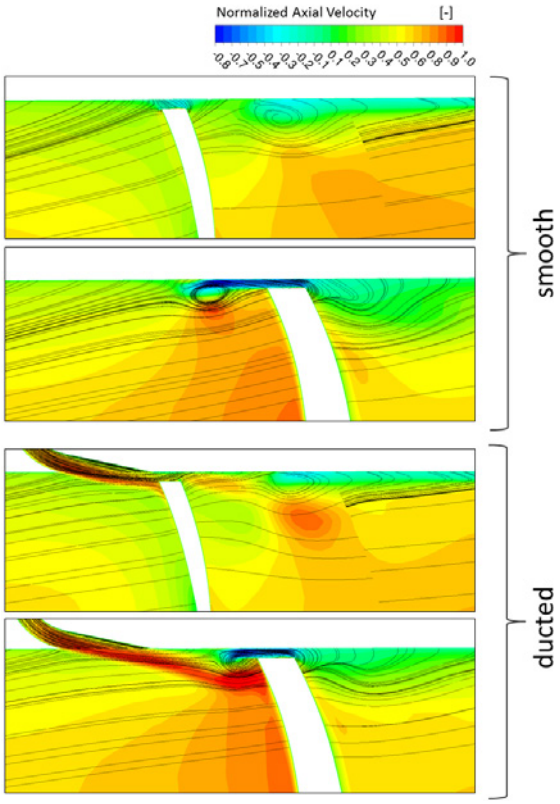

Figure 9. Axial Velocity Contours at NSP for Ducted and Smooth Casing Configuration at two different Points in Time

When the leading edge of the rotor blade passes the duct outlet, the recirculated fluid flows through the rotor tip gap in a positive axial direction, i.e. from the suction side to the pressure side of the blade. The injected jet streams out of the duct with a velocity in the order of the stage air intake speed and has a high axial velocity component. Additionally, the displacement effect of the stage mass flow causes the jet to run parallel to the shroud. While at the ducted configuration the high axial momentum of the jet prevents the equalizing movement of fluid from pressure side to suction side, at the smooth casing configuration a backflow through the gap has already developed, as can be seen in Fig. 9 (top). In this figure the axial velocity contour plot for the near stall operating point at two different time steps at a locally constant axial plane (equal to the plane in Fig. 7 and Fig. 8) is shown for each configuration. The corresponding line legend has been normalized with the maximum plotted velocity. Each contour is plotted in the same range. Besides, black-colored surface stream lines are plotted. For each configuration the top image shows the moment when the rotor leading edge just entered the plane. The bottom images show the situation only a few milliseconds later. The snapshots are taken while the front fifth of the rotor blade passes the plane. The comparison of the associated images clearly shows how the recirculated jet shifts the formation of the tip leakage vortex to a more downstream position. At the smooth casing configuration a tip leakage flow forms at the very front of the blade. At the ducted configuration this early backflow movement is prevented due to the high axial velocity component induced by the recirculated mass flow. This observation is in accordance with the studies of Strazizar et al. [7] and Suder et al. [12], which state that the increase of axial velocity inside the gap is the key to stability improvement.

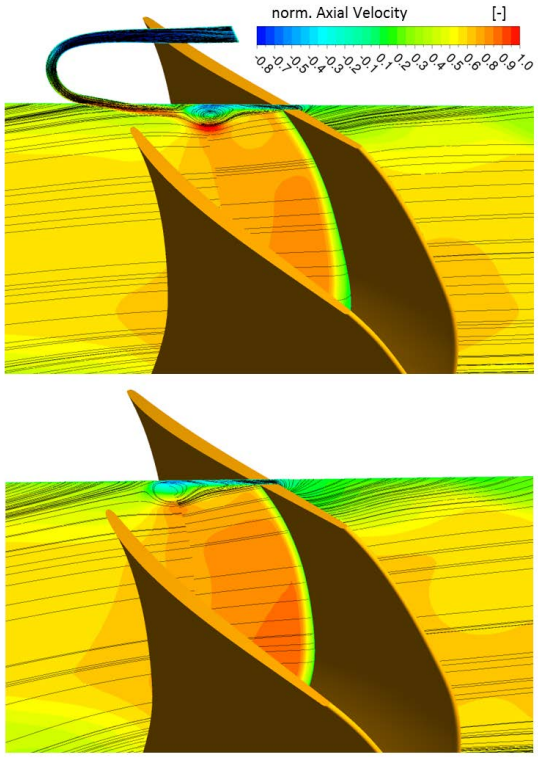

Figure 10. Axial Velocity Contours at NSP for Ducted and Smooth Casing Configuration

As the rotor leading edge moves further (Fig. 9 below), a backflow from pressure side to suction side also forms at the ducted configuration. On the one hand this is because the location of mass flow injection is further away from the tip gap and the tip blowing jet's axial momentum acting in the gap decreases. Another driving force is the comparatively high difference in pressure between pressure and suction side. The suppressed equalizing movement of the flow results in a higher pressure level in the tip region at the pressure side of the blade compared to the smooth casing configuration, which can be spotted in Fig. 7 and Fig. 8. As Bennington et al. declared, the bulk effects of the tip flow can be considered as a momentum

balance between the tip gap fluid and the approach flow [18]. So as soon as the force opposing the injected jet exceeds the force the jet induces in the gap, a leakage flow forms. Comparing the same instant, the circumferential propagation of the leakage flow and the resulting leakage vortex is smaller regarding the ducted configuration. The counteracting of the two effects can be seen in Fig. 10. In this figure the axial velocity contour in the previously considered plane is shown at an instant when the duct outlet is located in the middle of the rotor blade passage. Streaming into the blade channel, the jet runs parallel to the shroud, as it is displaced by the main flow. Concurrently the incoming jet also has a blockage effect, which leads to an evasive movement and therefore to a local axial acceleration of the main flow. Reaching the vortex region, the tip blowing jet splits into two parts. The upper part axially stagnates at the shroud and the lower part evades underneath the vortex. The acceleration of the evading mass flow contributes to the higher rotational velocity, which has been observed in Fig. 7 and Fig. 8.

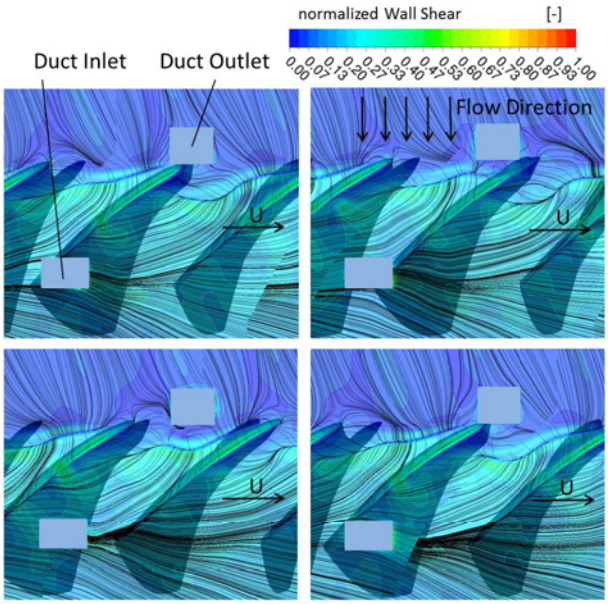

Figure 11. Position of Vortex Trajectory for four different Rotor Positions, NSP

2.4 Impact of Tip Blowing Jet on Vortex Shape

Fig. 11 shows the rotor domain of the ducted configuration at the near stall operating point at four different relative positions of duct and rotor blade. Plotted in this figure is the normalized contour of wall shear stress as well as the wall shear stress lines at the shroud. Due to the transparent view of the shear stress contour, the rotor blades, which pass the recirculation duct inlet and outlet, can still be seen. The converging shear stress lines, forming a continuous curve, show the separation line of the flow at the casing. After seperating from the casing, the tip leakage flow rolls up and forms the tip leakage vortex. On the basis of Fig. 11 the impact of the tip blowing mass flow on the course of the separation line becomes apparent.

As the rotor leading edge passes the duct outlet, the tip gap experiences an additional momentum in axial direction, which causes the separation line and therefore the location of vortex formation to shift downstream. The propagation of the tip leakage flow in circumferential direction is reduced, as can also be seen in Fig. 9 and Fig. 10. As the rotor leading edge leaves the influence area of the duct outlet, the location of vortex formation shifts back upstream. The recirculated mass flow causes a bump in the vortex shape which over time moves downstream. This results in a vortex shape which is highly variable in time. These observations are consistent with those of Khaleghi [15]. The temporal change of the separation line is depicted in Fig. 12. The shapes for the smooth casing and the ducted configuration are plotted in one diagram for the design point (top) and the near stall operating point (bottom). Both diagrams are plotted in the same range. The average shape of the separation line was calculated on the basis of the shapes in fifteen equidistant time intervals and is each shown as a bold line in the diagrams. To illustrate the variability of the vortex but keep the plot clearly, only three time-accurate lines per configuration and operating point are shown. These lines are depicted as thin lines, having the same color as their time-averaged counterparts. It should be noted that the diagrams do not show the complete shape for every evaluated point in time. As the position of beginning and ending of the separation line is changing with time, for some pionts in time the front or rear part is not shown. The downstream moving of the bump can be noticed for design conditions as well as for near stall conditions. However, for the near stall point the bump is much more distinct, which is due to the higher tip blowing mass flow and the smaller distance between the duct outlet and the location of vortex formation. The course of the separation line for the smooth casing configuration is not constant either. It fluctuates due to the wakes of the IGVs.

As expected, the mean course of the tip leakage vortex is located further upstream at the near stall operating point. A further throttling of the stage would lead to a further shift of the vortex in the upstream direction, until the vortex runs upstream of the rotor leading edge plane and the leakage flow spills into the adjacent passage. This forward spilling of the leakage flow is associated with the inception of spike type stall. Tip blowing causes the vortex to shift downstream and therefore delays the forward spill to lower mass flow rates. While the shift at design conditions is rather small, it increases with decreasing mass flow rate. Again, this can be explained by the higher tip blowing mass flow and the smaller distance between the duct outlet and the location of vortex formation at near stall operating conditions. The downstream shift of the mean tip leakage vortex is highly beneficial concerning the increase in stall margin.

2.5 Recirculated Mass Flow

The time-dependent mass flow through the inlet and the outlet of the recirculation duct as well as the corresponding relative positions between rotor blades and duct are shown in Fig. 13. In the graphic the inlet and outlet mass flow during

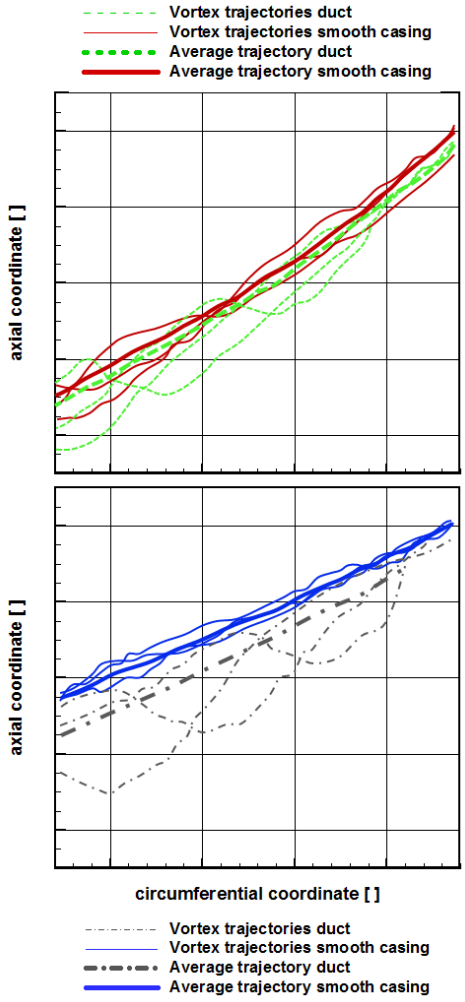

Figure 12. Position of Vortex Trajectories at DP (above) and NSP (below) for Ducted and Smooth Casing Configuration

design conditions and near stall conditions are plotted over the timestep number. As it takes 75 timesteps until one rotor passage has passed the recirculation duct, the flow pattern repeats every 75 timesteps. To enable the allocation of mass flow and relative position between duct and rotor blade the snapshots and the associated timesteps are marked. The six snapshots show a bird's eye view of the rotor blades (orange) and the associated position of the recirculation duct inlet and outlet (black), whereas the duct outlet has a square shape and the duct inlet has a trapeze shape. Apparently the mass flow varies depending on the rotor position, whereas the run of the curves representing the inlet mass flow and the outlet mass flow are phase-shifted. The region of high mass flow concerning the fluid extraction as well as the tip blowing extends over a relatively wide area, whereas the regions of low mass flow are characterized by a peaked minimum.

At the near stall operating point the maximum tip blowing jet is obtained when the duct outlet stands near the middle of the blade passage (snapshot 4). As soon as the duct outlet reaches the part of the passage which is mainly influenced by the pressure side of the blade, the tip blowing jet abruptly decreases. The jet starts to increase again as soon as the leading edge reaches the duct outlet (snapshot 5 and 6). While the suction side of the blade passes the duct outlet the tip blowing jet stays at a nearly constant level.

The phase-shifted mass flow of the extracted fluid reaches its maximum when the trailing edge of the rotor blade passes the duct inlet (snapshot 2). While the suction area passes the duct inlet the mass flow decreases. Entering the pressure area it increases again. The deviation from the average recirculated mass flow in the near stall operating point is up to 13%. Apparently there is a strong connection between the time-shift of the two mass flows and the circumferential distance between leading and trailing edge of the rotor blade and the circumferential distance between the recirculation duct inlet and outlet. Due to the lower static pressure ratio the

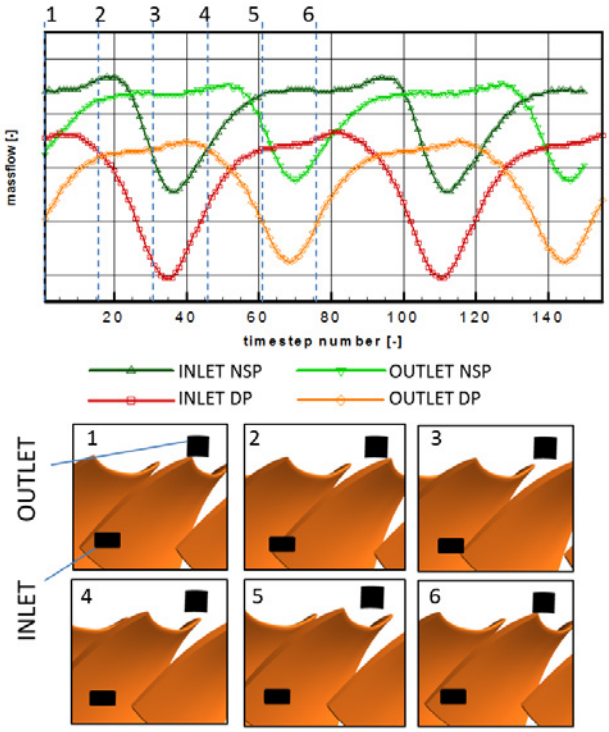

Figure 13. Mass Flow Rates at Inlet and Outlet of the Recirculation Duct

recirculated mass flow decreases with increasing stage mass flow. As the mean recirculated mass flow relative to the stage mass flow at the two calculated near stall operating points is 0.559% and 0.571% respectively, it decreases to 0.444% at design conditions and to 0.307% at the operating point on the choke side of the characteristic.

The position of the peak value concerning inlet and outlet mass flow shifts with changing operating conditions. While the position of minimum mass flow remains at a nearly constant location, the position of maximum mass flow changes. In comparison to the peak at near stall conditions, at design conditions the maximum tip blowing jet is achieved when the suction side of the blade surface is located more closely to the

duct outlet (snapshot 3). As the minimum is reached at the same relative position, the subsequent decrease of mass flow happens with a higher rate of change at near stall conditions. Since the same trend exists for the following increase of mass flow, the area of high mass flow is smaller at design conditions. These differences can be explained by the varying pressure distributions along the rotor blades and in the rotor passage. The characteristic of pressure and suction side, which changes with varying operating conditions, has an effect on the mass flow in the recirculation duct.

3. CONCLUSIONS

In the present study the impact of discrete tip blowing using recirculation ducts on the aerodynamic performance of a 1.5-stage axial compressor was numerically analyzed for a Rotor TCL of 1.7%. To take account of the fact that the rotor blades pass the duct inlet and outlet, time-accurate flow simulations were conducted. In addition to the effect of tip blowing on the efficiency and the operating range, a closer look was taken at the interaction between the tip blowing jet and the tip leakage vortex. The main conclusions can be summarized as follows:

- The examined recirculation ducts have an improving effect on the surge margin. A comparison with experimental data of 1% and 3% TCL showed, that the positive impact of the recirculation ducts increases with increasing TCL. When the TCL falls below a critical value (about 1% in the investigated setup) there is a predominant negative impact on the efficiency.

- Concerning the most throttled operating point available, a gain in efficiency of 0.19% is reached. While the aerodynamic properties of the near stall operating points improve due to tip blowing, a negative effect is recorded concerning the choke area of the characteristic as well as the design point. The achieved pressure rise of the ducted configuration is equal or even higher compared to the pressure rise of the smooth casing configuration. But regarding the efficiency in this area, recirculation has a deteriorating impact. At design conditions a decrease in efficiency of 0.17% is recorded.

- Tip blowing leads to a reduced deflection at the rotor tip area and to a slightly higher deflection at the rest of the blade. As the inlet flow angles do not change, this implies a shift of the aerodynamic loading from tip to hub.

- Due to the high axial velocity component of the tip blowing jet and the displacement effect of the main flow, the jet stays attached to the casing.

- The high axial momentum of the jet, acting in the tip gap at the leading edge of the blade, prevents the equalizing movement from pressure side to suction side. Thus the tip leakage flow forms at a more downstream position.

- Even if the tip leakage flow has evolved, the momentum of the jet directly counteracts the circumferential expansion of the leakage flow.

- Concerning the circumferential direction, the tip blowing jet successfully prevents the tip leakage vortex from rapidly propagating into the blade passage and causes a higher rotational velocity of the vortex.

- The impact of tip blowing on the aerodynamics is much less distinct at the design point than at near stall conditions. One reason for this is the lower amount of recirculated fluid. Another reason is the fact that at lower mass flow rates the tip leakage vortex forms at a more downstream position. In this case the distance between the origin of the vortex and the counteracting tip blowing jet is larger. Especially the combination of these two facts, lead to a small impact of tip blowing at low mass flow rates. Regarding the tip gap at the leading edge during design conditions, the jet is acting at a location where it is not required. Thus the losses produced by recirculating the flow overweight the aerodynamic enhancements. To improve the performance at design or near choke conditions, a downstream shift of the duct inlet might be useful.

- Tip blowing causes the tip leakage vortex to shift downstream and therefore delays stall inception through forward spill to lower mass flow rates. The vortex trajectory of the ducted configuration is highly variable in time.

ACKNOWLEDGMENTS

The investigations presented in this paper were conducted within the European research and engineering project LEMCOTEC (Low Emissions Core-Engine Technologies) and were funded by Rolls-Royce Deutschland Ltd. & Co. KG. The authors gratefully acknowledge all the partners involved in this project.

REFERENCES

[1] C.S. Tan, E.M. Greitzer, and H.D. Vo. Criteria for spike initiated rotating stall. *Journal of Turbomachinery*, 130, 2008.

[2] S. Weichert. Tip clearance flows in axial compressors, stall inception and stability enhancement. *Dissertation, University of Cambridge, Department of Engineering*, 2011.

[3] C. Guinet, A. Inzenhofer, and V. Gümmer. Influencing parameters of tip blowing interacting with rotor tip flow. *ASME Turbo Expo, GT2015-42039*, 2015.

[4] M.D. Hathaway. Self-recirculating casing treatment concept for enhanced compressor performance. *ASME Turbo Expo GT-2002-30368*, 2002.

[5] G. Cassina, B.H. Beheshti, A. Kammerer, and R.S. Abhari. Parametric study of tip injection in an axial flow compressor stage. *ASME Turbo Expo, GT-2007-27403*, 2007.

[6] W. Wang, W. Chu, and H. Zhang. The effect of injector size on compressor performance in a transonic axial compressor with discrete tip injection. *Proceedings of the Institution of Mechanical Engineers, Part A: Journal of Power and Energy*, 0(0) 1-12, 2014.

[7] A.J. Strazisar, M.M. Bright, S. Thorp, D.E. Culley, and K.L. Suder. Compressor stall control through endwall recirculation. *ASME Turbo Expo, GT2004-54295*, 2004.

[8] B.H. Beheshti, K. Ghorbanian, B. Farhanieh, J.A. Teixeira, and P.C. Ivey. A new design for tip injection in transsonic axial compressors. *ASME Turbo Expo, GT206-90007*, 2006.

[9] B.H. Beheshti, B. Farhanieh, K. Ghorbanian, J.A. Teixeira, and P.C. Ivey. Performance enhancement in transonic axial compressors using blade tip injection coupled with casing treatment. *Proceedings of the Institution of Mechanical Engineers, Part A: Journal of Power and Energy*, 219:321–331, 2005.

[10] H. Khaleghi, A.M. Tousi, M. Boroomand, and J.A. Teixeira. Recirculation casing treatment by using a vaned passage for a transonic axial-flow compressor. *Proceedings of the Institution of Mechanical Engineers, Part A: Journal of Power and Energy*, 221:1153–1162, 2007.

[11] C. Guinet, J.A. Streit, H.-P. Kau, and V. Gümmer. Tip gap variation on a transonic rotor in the presence of tip blowing. *ASME Turbo Expo, GT2014-25042*, 2014.

[12] K.L. Suder, M.D. Hathaway, Thorp S.A., A.J. Strazisar, and M.B. Bright. Compressor stability enhancement using discrete tip injection. *Journal of Turbomachinery, January 2001*, 123:14–23, 2001.

[13] H. Khaleghi and J.A. Teixeira. Numerical study of discrete tip injection in a transonic axial compressor. *ASME Turbo Expo, GT-2010-23608*, 2010.

[14] M. Künzelmann, R. Urban, R. Mailach, and K. Vogeler. Active flow control at a 1.5-stage low speed research compressor with varying rotor tip clearance. *Proceedings of the Institution of Mechanical Engineers, Part A: Journal of Power and Energy*, Special Issue Paper, 2011.

[15] H. Khaleghi. Effect of discrete endwall recirculation on the stability of a high-speed compressor rotor. *Aerospace Science and Technology*, 37:130–137, 2014.

[16] L. Castillon, N. Gourdain, T. Guédeney, and F. Sicot. Evaluation of two unsteady numerical approaches for the simulation of multi-frequency turbomachinery flows. *European Transport Conference*, 2015.

[17] A. Arnone and R. Pacciani. Rotor-stator interaction analysis using the navier-stokes equations and a multigrid method. *Journal of Turbomachinery*, 118:679–689, 1996.

[18] M.A. Bennington, J.D. Cameron, S.C. Morris, C. Legault, S.T. Barrows, J.-P. Chen, G.S. McNulty, and A.R. Wadia. Investigation of tip-flow based stall criteria using rotor casing visualization. *ASME Conference Proceedings, GT2008-51319*, 2008.